Title

Longitudinal Macular Structure-Function Relationships in Glaucoma and Their Sources of Variability

Authors

Nouri-Mahdavi, Kouros
Fatehi, Nima
Caprioli, Joseph

Publication Date

2019-11-01

DOI

10.1016/j.ajo.2019.04.034

Peer reviewed

HHS Public Access

Author manuscript

Am J Ophthalmol. Author manuscript; available in PMC 2020 November 01.

Published in final edited form as:

Am J Ophthalmol. 2019 November ; 207: 18–36. doi:10.1016/j.ajo.2019.04.034.

Longitudinal Macular Structure-Function Relationships in Glaucoma and Their Sources of Variability

Kouros Nouri-Mahdavi, MD, MS, **Nima Fatehi, MD**, **Joseph Caprioli, MD**

Glaucoma Division, Stein Eye Institute, David Geffen School of Medicine, University of California at Los Angeles, Los Angeles, California

Abstract

Purpose: 1) Review central structure-function (SF) relationships in glaucoma; 2) compare contributions of within-session and between-session variability to total variability of macular optical coherence tomography (OCT) thickness measurements; and 3) test the hypothesis that longitudinal within-eye variability of central SF relationships is smaller than between-individual variability.

Methods: We reviewed the pertinent literature on central SF relationships in glaucoma. Thirty-eight eyes (20 normal or glaucoma subjects) had ×3 macular images per session over 3 sessions and superpixels thickness measurements for ganglion cell layer (GCL), ganglion cell/inner plexiform layer (GCIPL), ganglion cell complex (GCC) and full macular thickness (FMT) were exported. Linear mixed models were used for estimating contributions of between- and within-session variability to total thickness variability. 120 eyes with ≥3 10° visual fields (VFs)/OCT images were enrolled for the longitudinal study. We investigated within-eye longitudinal SF relationships (GCIPL thickness vs. VF total deviations) with a change-point regression model and compared within-eye with between-individual variabilities with components-of-variance models.

Results: In the cross-sectional study, between-session component contributed 8%, 11%, 11%, and 36% of total variability for GCL, GCIPL, GCC, and FMT. In the longitudinal study, between-individual variability explained 78%, 77%, and 67% of total SF variability at 3.4°, 5.6°, and 6.8° eccentricities ($P<0.05$). Structure-function relationships remained stable over time within individual eyes.

Conclusions: Within-session variability accounts for most of macular thickness variability over time. Longitudinal within-eye SF variability is smaller than between-individual variability. Study of within-eye SF relationships could help clinicians better understand SF linking in glaucoma and help refine progression algorithms.

Corresponding author: Kouros Nouri-Mahdavi, MD, MS, 100 Stein Plaza, Los Angeles, CA, 90095, USA, Phone: 310-794-1487, Fax: 310-794-6616, nouri-mahdavi@jsei.ucla.edu.

INTRODUCTION

Glaucoma is a major cause of visual disability, diminished quality of life, and blindness worldwide.[1] The hallmark of glaucoma is progressive loss of retinal ganglion cells (RGC) and their axons projecting information to the visual cortex. Spectral-domain optical coherence tomography (SD-OCT) has provided us with an unprecedented opportunity to monitor the RGCs and their neural processes, i.e., axons and dendrites, by measuring the thickness of the peripapillary retinal nerve fiber layer (RNFL), the neuroretinal rim at the optic nerve head or inner retinal layers in the macula.[2]

Damage to RGCs is expected to lead to loss of visual function. The subject of structure-function in glaucoma has elicited a great amount of interest in the glaucoma community.[3] Correlation of structure and function is helpful clinically to confirm and emphasize the topography and severity of glaucomatous damage at diagnosis. Simultaneous or sequential evidence of progressive RGC damage and corresponding visual field (VF) loss aid detection of disease deterioration and clinical decision making.

There is some redundancy in the RGC complement of the human eye so that damage on standard achromatic perimetry (white on white target) may not appear before some loss of RGCs has occurred. Quigley et al. found that VF sensitivity began to decline soon after the initial loss of RGCs in a sample of 6 cadaver eyes.[4] Within the central 30° of the retina, 5-dB and 10-dB sensitivity losses corresponded to about 20% and 40% RGC loss, respectively. In addition, they reported that up to 40% of RGCs could be lost before evidence of field loss could be established on standard achromatic perimetry. On the other hand, signs of VF loss can also manifest before definitive signs of structural damage. Visual field loss was the most frequent earliest sign of conversion to glaucoma in the European Glaucoma Prevention Study.[5]

There has been much discussion about the nature and strength of the relationship between RGC loss and functional deficits in glaucoma commonly referred to as the structure-function (SF) relationship. Most studies have explored SF relationships in pooled cross-sectional samples of patients. Linear and nonlinear relationships have been described that are likely related to the type of structural and functional measurements used, the scale in which outcomes of interest are expressed (such as linear or logarithmic), and the amount of inter-individual variability for those outcome measures.[3]

The advent of SD-OCTs ushered in a new era in glaucoma diagnostics and for the first time enabled us to accurately measure the thickness of retinal layers in the central macula. While evidence for early macular RGC damage had been detected in animals with experimental glaucoma[4] and was suspected based on functional measurements,[6] Zeimer and colleagues were the first investigators to demonstrate that evidence of retinal thinning could be detected clinically in the central macula in glaucoma.[7] About 30% of the RGC complement in the human eye is located within 16 degrees of the foveal center.[8] The macula is the only retinal region where the ganglion cell layer (GCL) is more than one cell thick with the peak RGC density (about 6–7 layers of RGCs) occurring 750 to 1100 μm from the foveal center.[9] The RGCs in the central macula are affected early during the disease[10,11] and at the same time,

are the last cells to be lost in glaucoma.[12,13] Hence, imaging of the macula with SD-OCT could provide clinicians with valuable information regarding the course of the disease at all stages of glaucoma.

There is evidence that measurement of the GCL or the GCIPL, the combined thickness of the GCL and inner plexiform layer (IPL) or the macular ganglion cell complex (GCC, the combined thickness of the RNFL, GCL, and IPL) can detect early glaucoma with a performance that approximates that of circumpapillary RNFL (cpRNFL) thickness measurements.[14–17] Macular thickness measures demonstrate a strong correlation with VF sensitivities comparable to that of cpRNFL thickness.[18] Also, a strong correlation has been reported between the macular GCIPL layer thickness and estimates of RGC counts.[19,20]

The role of macular imaging for detection of disease progression remains less well established and is the subject of ongoing investigations, although there is substantial evidence to support its utility. Of utmost importance with regard to detection of progression is the magnitude of variability for various macular outcomes of interest both within a measurement session (within-session variability) and between sequential measurement sessions (i.e., between-session variability). Ideally measurement variability should be minimized so that smaller amounts of change can be efficiently detected on follow-up testing. It is not clear, at this point, how much of the total variability seen on sequential imaging sessions is explained by within-session vs. between-session variability. In case most of the longitudinal variability over time is explained by within-session variability, one could argue that within-session variability should be measured at baseline and used as a yardstick for gauging individual variability in a given eye and for defining limits of variability for individual eyes.

Study of SF relationships in pooled cross-sectional samples of patients is of interest and has been the traditional approach used in the published literature; we propose that the study of SF relationships the macula. The inner macular thickness measurements vary significantly as a function of distance from the foveal center and hence, this variability needs to be taken into account when SF relationships are studied in the macula.

STUDY AIMS

The goals of the current study were: 1) to provide an overview of the SF relationships in the macula and propose a framework for studying central SF relationships within individual eyes; 2) to estimate and compare the relative contribution of within-session and between-session variability to total variability of macular superpixel thickness measurements; and 3) to test the hypothesis that within-eye variability of macular/central VF structure-function relationships is significantly smaller than between-individual variability as within-eye variability mostly represents measurement noise. We will provide proof of concept in support of studying *individual* SF relationships to better understand the nature of RGC damage in the central macula. The radially symmetric structural and functional measurements around the fovea or the VF fixation point are expected to demonstrate the same underlying SF relationship within an individual eye. Therefore, between-individual variability in SF relationships is likely the most important contributing factor to the total variability observed in cross-sectional SF studies.

METHODS AND PATIENTS

Both studies were approved by the Human Subject Protection Committee and the Institutional Review Board of the University of California Los Angeles. Subjects were prospectively consented. The studies were carried out in accordance with the tenets of the Declaration of Helsinki and the Health Insurance Portability and Accountability Act (HIPAA).

SUMMARY OF EVIDENCE REGARDING CENTRAL STURCTURE-FUNCTION RELATIONSHIPS IN GLAUCOMA

We reviewed the pertinent literature regarding utility of central SF relationships in glaucoma.

CROSS-SECTIONAL STUDY SAMPLE

Thirty-eight eyes of 20 normal subjects or patients with glaucoma were prospectively enrolled. The glaucoma eyes were diagnosed by one of the authors (KNM, JC) and had glaucomatous optic neuropathy and reproducible VF loss as detailed below.[21] Normal subjects had no history of ocular disease, open angles, and normal optic nerve and retinal nerve fiber layer on dilated fundus exam. After a complete eye exam, the subjects underwent macular SD-OCT imaging as described below. Three macular images were acquired at each of three different sessions within 3 months by one operator with Spectralis OCT. The SD-OCT images were segmented with the Glaucoma Module Premium Edition (GMPE) software of Spectralis OCT and the thickness of individual layers or combination of retinal layers (GCL, GCIPL, GCC and FMT) was calculated for an 8×8 grid of 3°×3° superpixels aligned horizontally (Figure 1). The central 36 (6×6) superpixels of the 8×8 grid were used for the cross-sectional part of the study as we have previously shown that the most peripheral superpixels of the macular cube show the highest variability.[22]

LONGITUDINAL STUDY COHORT

One hundred twenty glaucoma eyes (from 120 patients) with 3 or more 10–2 standard achromatic VFs and macular SD-OCT images and ≥30 months of follow-up were enrolled from The Advanced Glaucoma Progression Study, a longitudinal prospective study underway in the Glaucoma Division, Stein Eye Institute. The eligible eyes had good quality macular SD-OCT images defined as quality factor >15 for all of the linear B-scans included in the central 24°×24° grid and no major artifacts on these B-scans on review of the images. Glaucoma was defined as the presence of glaucomatous optic nerve damage and an associated reproducible VF defect on standard achromatic perimetry. Eligible eyes were also required to demonstrate a VF mean deviation worse than −6.0 dB or involvement of the central 10° on the standard achromatic 24–2 VFs defined as presence of 2 or more points with P <0.05 on the pattern deviation plot. Other inclusion criteria included age 50–85 years, best corrected visual acuity ≥20/50, and no significant confounding retinal or neurological disease. Study eyes underwent a thorough eye exam at baseline including biometry with IOLMaster, cpRNFL and triplicate macular imaging with Spectralis SD-OCT (Heidelberg Engineering®, Heidelberg, Germany), and SITA standard 24–2 and 10–2 VFs with Humphrey Field Analyzer (Carl Zeiss Meditec®, San Leandro CA).

IMAGING PROCEDURES

The macular imaging algorithm of the Spectralis OCT (Posterior Pole Algorithm) consists of 61 horizontal B-scans (repeated 9–11 times to improve image quality) each consisting of 768 A-scans spanning a 30°×25° wide area centered on the fovea. After segmentation of individual layers, the data are averaged and an 8×8 grid of thickness measurements (64 superpixels within the central 24°×24°, 3° wide squares) for the layer of interest is created (Figure 1). The GMPE software is able to segment all the individual retinal layers. The main macular structural outcomes of interest were GCL, GCIPL, GCC, and FMT in the cross-sectional study and GCIPL thickness in the longitudinal study as we have shown this parameter to have the highest correlation with pointwise central VF sensitivities.[23] The layer segmentation results were checked and manually corrected on the SD-OCT images as needed.

For the longitudinal part of the study, GCIPL measurements at 64 superpixels from the Posterior Pole Algorithm and total deviation (TD) values for the 68 test locations from the 10–2 VFs were exported and matched topographically adjusting for ganglion cell displacement (Figure 2A). Although the macular images are acquired along the fovea-Bruch's membrane axis, the GMPE software allows for measurement of the superpixels in a horizontally aligned grid so that the superpixels represent the exact same locations across different eyes. Corresponding data from the central 18° of the macula and VF were included for further analyses since beyond this eccentricity, the thickness of the inner macular layers rapidly decreases (Figure 2B). GCIPL thickness valued were converted to log scale ($\log GCIPL = \log_{10} GCIPL$) so that they are expressed in the same scale as VF data.

VISUAL FIELD EXAMINATION

The patients in the longitudinal part of the study underwent central 10° VF tests (10–2) performed every 6 months. The 10–2 strategy of the Humphrey Field Analyzer measures VF sensitivity at 68 test locations, 2° apart on vertical and horizontal axes, within 10° of the fixation point. Since both SD-OCT and VF measurements are based on distance in degrees from the fovea or fixation point, such measurements can easily be overlaid (Figure 2). The VF test locations in Figure 2 were adjusted for displacement of RGCs in the central macula according to Raza and colleagues based on Drasdo et al.'s estimations of average displacements in normal subjects.[24,25]

STATISTICAL METHODS

Cross-sectional study—The pairwise absolute difference between the 9 thickness measurements available for all the central 36 superpixels in each eye were calculated. The average absolute difference and the 95% confidence intervals were plotted and compared for the 4 macular outcomes of interest with Kruskal-Wallis test. The distribution of the limits of variability as a function of superpixel location was investigated qualitatively on scatter plots **of absolute differences in thickness against superpixel location**. Linear mixed models were used to estimate the relative contributions of between-session and within-session variability to total variability for macular outcomes of interest (i.e., GCL, GCIPL, GCC, and FMT). Diagnosis **(glaucoma vs. normal)** and location of superpixel were used as fixed-effect variables; imaging session and patient ID were fitted as the variables with random

effects in this model. The ratio of between-session variability to total variability was then calculated.

Longitudinal study—Bivariate plots for SF relationships for each individual eye were drawn at baseline with the logGCIPL thickness at superpixels on the Y-axis and the TD values at matching individual test locations on the X-axis. Total deviation values represent differences between measured sensitivity at a test location and the average age-corrected normal thresholds for the same test location. Fifty-three eyes in which the range of structural and functional measurements extended throughout most of the dynamic range for both measures were selected after a qualitative review of the plots by one of the investigators (KNM). The SF plots were then separately studied in these 53 eyes as a function of distance from the fovea at 3 eccentricities of roughly 3.4° **(4 superpixels)**, 5.6° **(8 superpixels)** and 6.8° (**12 superpixels)** (Figure 2B) so as to address the variability of thickness measurements with changing distance from the fovea.[23] From the 53 eyes, only those with at least 4 sessions for circle 1 (3.4° eccentricity), and at least 3 sessions for circles 2 and 3 (5.6° and 6.8° eccentricities) were **included in the analyses** to have a minimum of 16 points for regression analyses as there are only 4 points available per eye per session at 3.4° eccentricity as opposed to 8 points at 5.6° eccentricity and 12 points for 6.8° eccentricity. The GCIPL measurements were transformed into logarithmic scale as the TD values are expressed in logarithmic scale (dB).

A change-point mixed effects regression model (also known as the broken-stick model) was used to investigate the SF relationships within each individual eye. The broken-stick model assumes that within the dynamic range of OCT measurements, i.e., between the OCT measurement ceiling and measurement floor, there is a direct linear relationship between structure (OCT thickness at each superpixel) and function (TD at each corresponding 10–2 VF test location). After OCT measurements reach their floor, this relationship changes to a flat line with virtually no change in structure despite ongoing changes in function. This model can also investigate whether each eye displays a different SF relationship at different sessions or if the regression slope is constant over time.

The change-point regression model of Y = $\log_{10}$GCIPL vs. X = TD as a function of eccentricity or distance from the fovea is of the form

$$\mathbf{Y_{ij} = a_i + I\left(b_{0i} + b_i X + d_i * session + f_i * X * session\right) + e_{ij}}$$

where

I = 1 if X > C_i and I = 0 if X ≤ C_i;

C_i the break-point (change-point) for the i^{th} eye;

e_{ij} is within eye error;

a_i is the intercept for the i^{th} eye;

b_{0i} is the change in the intercept if X > C_i for the i^{th} eye

b_i is the slope for logGCIPL in units of log(μm)/dB for the ith eye;

d_i is the change in Y per session for the ith eye; and

f_i is the change in the logGCIPL slope due to session (TD-session interaction) for the ith eye.

If there is no upward or downward displacement of the SF relationship curve over multiple testing sessions, then its coefficient d would be equal or very close to 0 and f would be equal to 0 on average. If the GCIPL slope does not change over sessions, then the coefficient for the interaction of TD (X value) and session (f) would be 0 on average. An attempt to estimate the variances of a_i, b_{0i}, b_i, c_i, d_i and f_i assuming normal distribution and using a maximum likelihood approach was unsuccessful; in statistical terms, the model did not converge. Therefore, a broken-stick model was fit to each eye where the values were estimated for each eye. This method does not require **any of the parameters** to follow any known distribution such as the normal distribution. However, in this analysis, we required the change-point (C_i) not be **above −5 dB** based on prior data.[23]

If the minimum TD was >–5 TD units, we assumed that the TD data are all above (i.e., are beyond) the true break-point and the break-point could not be estimated from the data. In this case, only the slope of logGCIPL against TD (but not the intercept) can be estimated. To measure the contributions of within-eye vs. between-individual variation to the total variability observed in this sample, we defined the components of variance as follows.

$$\textbf{Total variance of Y} = \textbf{within-eye variance} + \textbf{between-eye variance}$$

The variance of the residual errors (e_{ij}) is the same as the within-eye (within-model) variance. If $\hat{Y}_{ij}$ is the predicted value for a given eye "i" and observation "j", the variance of $\hat{Y}_{ij}$ represents the between-eye (between-model) variance. The intraclass correlation coefficient (ICC) is defined as the ratio of the between eye variance to the total variance under the above change-point regression model. It varies between 0 and 1 with a value closer to 1 indicating larger variability due to differences between different subjects explain a higher proportion of the total variability compared to within individual eyes.

RESULTS

CROSS-SECTIONAL STUDY

Table 1 summarizes the demographic and clinical findings of the enrolled eyes in the cross-sectional study. Twentysix eyes of 14 glaucoma patients and 12 eyes of 6 normal subjects were included in the cross-sectional study. The mean absolute difference in thickness at superpixels among the 9 set of SD-OCT images were 1.2 (±0.6), 1.6 (± 0.6), 1.8 (± 0.8) and 1.7 (± 0.7) μm for GCL, GCIPL, GCC and FMT, respectively. Figure 3 displays boxplots comparing the mean and 95% confidence intervals for the 4 macular parameters. The GCL demonstrated the lowest and GCC had the highest overall absolute thickness differences. All the pairwise differences between the macular outcome measures were statistically significant (P <0.001, Kruskal-Wallis test). The ratio of variance to average thickness decreased with increasing thickness of the layer of interest (GCL > GCIPL > GCC > FMT, P <0.05,

Kruskal-Wallis test). The superpixel location across the macula did not seem to have a systematic effect on thickness variability (Figure 4). The contribution of between-session variability to total variability was lowest for GCL (8%) and increased to 11% for GCIPL and GCC and 36% for FMT, respectively (Figure 5). This means that most of the total observed variability over time could be explained by within-session variability.

LONGITUDINAL STUDY

One hundred twenty eyes with 3 or more sessions of macular SD-OCT imaging and 10–2 VF exams were eligible for the initial screening. Cross-sectional SF relationships were then plotted for individual eyes at baseline. Figure 6 depicts scatterplots demonstrating the relationship between the GCIPL thickness at superpixels and TD values at individual test locations on the central 10–2 VF for representative individual eyes. Three main patterns were observed depending on the severity of the glaucomatous damage at the level of macula and central field. The scatterplot on top left displays a typical broken-stick pattern, since both GCIPL thickness and VF sensitivity values vary through most or all of their entire range of measurements. On the top right scatterplot, the GCIPL thickness measurements vary through most of their dynamic range, whereas there is limited variability in VF measurements, indicating that there was only mild corresponding VF damage. On the bottom image, the VF threshold values demonstrate a much wider range of variation in contrast to the GCIPL thickness as the latter has reached its measurement floor.

Fifty-three eyes in which the bivariate plots demonstrated structural and functional measurements to vary through most of or the entire dynamic range were selected for further analyses (Table 2). The average (±SD) mean deviation of the 10–2 VFs in this select group was −9.7 (±4.9) dB and there was a median (IQR) of 4 (4–6) SD-OCT images and VF exams per eye over a median (IQR) follow-up time of 2.4 (2.2–2.9) years. The average GCIPL thickness was 56.0 ± 15.3, 63.4 ± 17.9, 49.0 ± 11.2 μm for superpixels at 3.4°, 5.6°, and 6.8° eccentricities.

Based on our previous work[23] and additional preliminary analyses, we limited the break-point to be equal to or lower than −5 dB as mentioned above. The useful range of macular structural measures does not exceed one log unit of TD change (10 dB). This is consistent with findings by other investigators and our laboratory on other structural measures such as the cpRNFL and Bruch's membrane based minimum rim width thickness.[26–28] Table 3 summarizes the results of the 53 segmented (broken-stick) regression analyses in this group of patients as a function of eccentricity. Overall, our assumption of stability of SF relationships over time seemed to hold as there was no significant interactions between the TD and session in any of the models, nor was the session effect significant for any eccentricity ($P \geq 0.057$). A review of the broken-stick model fits revealed the following reasons some models could not be fit. In some eyes, the data below −10 dB of TD were limited and therefore, the change-point (C) confidence limits were large. Presence of outliers was another possible confounding factor as we did not attempt to remove outliers in this study. Therefore, significant residual variability was observed in some eyes. Figure 7 demonstrates examples of longitudinal structure-function relationships in individual eyes.

The estimated ICCs for comparison of longitudinal within-eye variability to between-individual variability in SF relationships were 0.780 (95% CI: 0.728–0.818), 0.766 (95% CI: 0.727–0.800), and 0.665 (95% CI: 0.607–0.723) at 3.4°, 5.6°, and 6.8° eccentricities, respectively. As the ICCs for all eccentricities significantly exceeded 0.5, we can conclude that within-eye variability was significantly smaller than between-individual variability at all eccentricities although the within-eye variability component was significantly lower for the 3.4° and 5.6° eccentricities compared to 6.8° eccentricity. Figure 8 depicts the *median* broken-stick or change-point model in this group of patients. While the slopes for 5.6° and 6.8° eccentricities were parallel with a higher intercept for 5.6° eccentricity, the slope for the 3.4° eccentricity was less steep with the measurement floor (intercept) between the two farther eccentricities. A formal comparison with Wilcoxon signed rank test showed that the intercepts were different among the 3 eccentricities; the *P* value was <0.001 for the pairwise comparison of 5.6° eccentricity against 3.4° and 6.8° eccentricities whereas the *P* value for comparison of 3.4° eccentricity vs. 6.8° eccentricity was 0.033. The *P* values for pairwise comparison of slopes at 3.4° vs. 5.6°, 3.4° vs. 6.8°, and 5.6° vs. 6.8° eccentricities were 0.149, 0.701, and 0.136, respectively.

DISCUSSION

STRUCTURE-FUNCTION (SF) RELATIONSHIPS IN GLAUCOMA

The topic of SF relationships in glaucoma has been a subject of great interest since the development of automated imaging devices such as scanning laser ophthalmoscopy, scanning laser polarimetry and more recently OCT. At the most basic level, one would expect that a reduction in the number of RGC axons would be consistent with visual functional loss measured with various devices on some scale; perimetry has been the most commonly used technique for measuring visual function in structure-function studies in glaucoma.

Lessons learned from structure-function relationships with SD-OCT cpRNFL measures—Numerous studies have investigated the relationship between global and sectoral cpRNFL thickness measurements derived from SD-OCT and corresponding parameters from standard achromatic perimetry. These studies showed that SF relationships do not show complete agreement, vary as a function of glaucoma severity, and can be improved if customized for individual eyes.[29–38] Perfect correlation of structure and function is not expected nor desirable as this would mean that structural measures would not provide additional information beyond VF data or vice versa. Medeiros and coworkers proposed a SF index incorporating both cpRNFL thickness and VF sensitivity data that could be used to estimate the number of RGCs in an individual eye.[39] This index has been demonstrated to be able to stage glaucoma severity and estimate rates of change adequately compared to isolated measures of structure and function and possibly aid with detection of disease progression.[40–43]

While different approaches have been used to study SF relationships in glaucoma,[44–49] the most widely adopted model is the one called the simple linear model by Hood and Kardon.[26] This models posits that structural measurements, such as cpRNFL, consist of a neural

component, i.e., RGC axons, and a non-neural component, which consists of glial tissues, blood vessels and other connective tissue components. With progressing damage in glaucoma, the neural component thins out whereas there is no significant changes to the non-neural component or it could actually increase in thickness as proposed by Harwerth et al.[50] Therefore, the thickness of any OCT outcome measure, such as cpRNFL, never reaches zero and there is a measurement floor that varies according to the outcome of interest, the topography of damage, and the characteristics of an individual eye. Many studies reported that the cpRNFL thickness reaches its measurement floor after about a 10-dB decrease in threshold (i.e., an average sectoral mean deviation of −10 dB).[26–28] Circumpapillary RNFL thickness reaches a plateau at around this level of damage beyond which the amount of change is very small to none. The magnitude of the correlation between cpRNFL thickness measurements and VF threshold sensitivity or global or sectoral mean deviation values has been quite variable in the reported studies with a peak correlation of 0.70 to 0.80.[29–38]

Structure-function relationships in the macula—All SD-OCT devices are able to measure the macular layers with slightly different algorithms providing clinicians with thickness measurements for GCL, GCIPL, GCC, or full macular thickness (FMT) depending on the imaging and segmentation strategy used by the device. Macular SD-OCT outcome measures demonstrate high correlations with threshold sensitivity in the central VF similar to cpRNFL.[18,23,51,52] Central test locations of the 24–2 VF or 10–2 VF test locations measuring the sensitivity at 68 test locations within 10° from the fixation point have been used for this purpose. Overall, the strength of SF relationships in the macula seems comparable to those for cpRNFL thickness. Multiple studies including those from our research laboratory (see below) have confirmed this finding with correlation coefficients for global or local SF relationships reported as high as 0.6–0.75.[51,53–56] There is a one-to-one relationship in the macula between the local thickness measurements (or superpixels) and the threshold sensitivity or TD values at individual VF test locations (Figure 2). Thicker GCIPL or GCC measurements have been associated with higher threshold sensitivity in normal eyes.[57] Regional or local SF relationships for individual macular superpixels, sectors, or circular areas around corresponding VF test locations have been investigated.[51,23,25] The inferotemporal macular sector discriminates best between glaucoma and normal eyes.[15,16] The inferotemporal sector or inferior hemi-macula has been found to demonstrate the strongest association with VF thresholds.[15,16] Evidence of retinal thinning could also be detected in the hemi-macular region corresponding to the normal hemifield in eyes that showed VF loss only in one hemifield.[58,59] As with cpRNFL thickness, macular outcome measures reach their floor of measurements by the time 10 dB loss is registered at the corresponding test location. The advantage of macular SD-OCT measures over cpRNFL outcomes is that the macular RGC axonal complex persists until later stages of the disease and therefore, could be potentially used for detection of change over time. We explored correlations between TD measurements at 10–2 VF test locations and GCIPL thickness on a 100×100 array of superpixels derived from Cirrus high-definition OCT in 137 eyes of 125 glaucoma patients.[56] We reported that the macular GCIPL loss demonstrated an arcuate pattern, the topography of which depended on the corresponding location in the central field. We recently tested the hypothesis that measuring the GCL, where the RGC somas are located, would improve SF relationships and extend the range of utility of macular thickness

measurements.[23] We enrolled a cohort of glaucoma eyes from the Advanced Glaucoma Progression Study to compare the SF relationships and measurement floor among various macular outcomes of interest. We estimated localized SF relationships between macular thickness at superpixels and the VF TD values at corresponding individual test locations on 10–2 VFs in 96 glaucoma and 10 normal eyes and measured the dynamic range of structural measurements.[23] We analyzed the central 24 superpixels located in the central 18° of the macula and the corresponding VF test locations after correcting for RGC displacement. Beyond the central 18° from the fovea, the thickness of many inner retinal layers significantly decreases to very low levels.[60] Structure-function plots were constructed as bivariate plots with the TD values at individual test locations on the X-axis and various macular thickness measures (in μm) on the Y-axis. Based on nonparametric correlation analysis between macular measures and VF TD values, SF relationships were strongest for GCIPL, GCL, and GCC in that order (Spearman's ρ =0.669, 0.654, and 0.638, respectively); however, the differences were not clinically meaningful. We then used a broken-stick model to fit the SF data.[26,61] A broken-stick model in the form of $\mathbf{Y = a \text{ if } X < C, Y = a + b\,(X-C) \text{ if } X \geq C}$, was fit to the cross-sectional SF data where *a* is the intercept (an estimate of the measurement floor for macular outcome measures) in μm, *b* represents the slope beyond the change-point in μm/dB, and *C* denotes the VF threshold at the change-point (Figure 9). The model posits that beyond the change-point, the macular thickness is linearly correlated with the corresponding TD values. The dynamic range was considered to be the difference between the intercept for the broken-stick model (i.e., the bottom of measurements), and the 90th percentile normal thickness as the measurement ceiling.[27] Figure 9 demonstrates a plot of *predicted* macular IPL, GCL, GCIPL, GCC and FMT (i.e., predicted *y*'s) at superpixels against VF TD at corresponding individual 10–2 test locations.

The variability of any given macular parameter needs to be considered compared to its dynamic range and not in comparison to the total measurement range. As mentioned above, with both macular and cpRNFL measurements, there is a lower plateau or measurement floor below which the measurements almost never drop.[27,61,62] The absolute dynamic range of measurements in the above study was a function of the average layer thickness in normal subjects and was highest for FMT, followed by GCC, GCIPL, and GCL in that order (Table 4). However, inner macular outcome measures had the highest *relative* dynamic range (GCL > GCIPL > GCC in that order). The change-points were similar for all outcome measures ranging between −7.8 and −8.9 dB. As the variability of all macular outcome measures is uniform across the macula with current technology,[22] GCL measurements may not provide added value compared to GCC or GCIPL at this point. However, given the higher relative dynamic range for GCL, this issue deserves further exploration with longitudinal data.

A shortcoming of available SF studies is that the associations observed are highly dependent on the level of structural and functional damage, the number of eyes recruited and inclusion of normal and glaucoma suspect subjects in addition to glaucoma patients. From a statistical point of view, a significant amount of the association observed is driven by points at the two ends of the data cloud (i.e., those with lowest and highest X values); in addition, in studies that use a change from average normal values, these average values for thickness or sensitivity measurements have large 95% prediction intervals and do not necessarily

represent the true amount of change from baseline for any individual eye at any given point in time; the above factors highly affect the strength and the pattern of correlation observed in a study and therefore, comparison across studies can be very challenging. A more meaningful type of correlation analysis would be to compare a change from baseline in structure to a change from baseline in function. This type of comparison obviates some of the shortcomings mentioned above and can provide a better insight into the relationship between structure and function. Our research laboratory is actively investigating this topic at the time of this writing.

DETECTION OF DISEASE PROGRESSION WITH MACULAR SD-OCT IMAGING

Given that SD-OCTs have been in clinical use for a relatively short time, only preliminary data are available regarding the performance of macular SD-OCT measurements for detection of glaucoma worsening.[63–66] Sung et al. showed that rates of progression for macular full thickness measurements were significantly higher than cpRNFL rates of changes in eyes progressing based on VF or optic disc criteria.[63] The average baseline VF mean deviation was −14 dB in that study. None of the cpRNFL rates was significantly different from zero. Lee and associates reported similar findings using event analyses in a group of glaucoma eyes mostly (90%) composed of normal tension glaucoma patients.[65] Na and colleagues found that the optic nerve head, cpRNFL, and macular parameters all showed a faster rate of progression in deteriorating glaucoma eyes compared to stable eyes.[64] Suda et al. demonstrated that the longitudinal noise of GCC measurements was comparable to cpRNFL measurements in a group of eyes with moderate glaucoma (average MD =−6.2 dB)[66]; however, the correlation of structural rates of progression with perimetric rates of change was weak. Hammel and associates reported that, in a subset of eyes with severe glaucoma (20 eyes), the average normalized GCIPL rates of change were higher (–1.8%, 95% CI: −3.6%, – 0.01%) than average ppRNFL rate of change (–1.1%, 95% CI: −2.4%, 0.3%).[67] Lee and associates found that the average GCIPL thickness in the hemimacular area corresponding to the affected hemifield showed significantly faster rates of thinning in eyes progressing according to VFs and ONH/RNFL photographs compared to stable eyes.[68]

MEASUREMENT VARIABILITY OF MACULAR THICKNESS MEASUREMENTS

Within-session and inter-session reproducibility of SD-OCT parameters are important as far as detection of change over time is concerned. The reproducibility of various macular thickness parameters has been shown to be excellent.14,22,69,70 Although the magnitude of within- and between-session variability has been reported for larger regions of the macula, the relative contribution of these two components of variability have not been previously reported for macular outcomes. In a study by Tan et al., both GCC and macular full thickness measurements were highly reproducible with ICC ≥0.98 for all measures.[71] In another study, ICCs for repeated measurements within the same session were 0.995, 0.994, and 0.989 for the average, superior hemiretinal, and inferior hemiretinal GCC thickness, respectively.[72] Within-session test-retest variability values, defined as the 95% boundaries for variability, were 3.6, 5.0, and 4.1 μm for the same parameters. The corresponding coefficients of variation (CoV) were also very low (2.1%, 2.9%, and 2.4%, respectively). Mwanza and colleagues found that GCIPL measurements showed excellent reproducibility and suggested that this parameter could be used for detection of structural progression.[69]

Hirasawa and colleagues reported high reproducibility for GCC and GCIPL layers with 3D OCT-1000 with CoVs that were <1% for all regional and global measures.[70] Kim and colleagues investigated macular thickness variability over time in 109 glaucoma eyes that were considered to be clinically stable.[73] They confirmed that variability was very low for all GCIPL-derived parameters. They also found that worsening glaucoma severity, i.e., thinner baseline GCIPL, did not affect between-session variability. Francoz et al. reported that between-session variability was very low in seemingly stable glaucoma eyes over wider sectors of the macula.[76]

Measurement variability is expected to vary across the macular region depending on its topography and to be higher in smaller areas of the macula. In a recent study, we used the Posterior Pole Algorithm of the Spectralis OCT to estimate within-session thickness measurement variability in 123 glaucoma and normal eyes at the level of 3°×3° superpixels.[22] We found that the local within-session variability was excellent and did not exceed 3 μm for all macular parameters (IPL, GCL, macular RNFL, GCIPL, GCC, and FMT) after excluding a small percentage of outliers. This excellent repeatability (lower than the 4 μm nominal axial resolution of Spectralis OCT) is explained by averaging of data and the fact that the software uses all available 3-D information when segmenting the inner retinal layers.[74,75] Any change beyond the cutoff point for within-session variability as defined in this study (about 3 μm), would be of potential clinical significance assuming that between-session variability does not exceed within-session variability significantly, an issue investigated in this thesis. We found that variability was highest on the nasal and superior columns/rows of superpixels on the macular images. The size of superpixels on the Posterior Pole Algorithm was empirically chosen to be 3°×3° degrees by the manufacturer. Our unpublished data previously showed that variability increased as the size of the area of interest decreased. However, this relationship may not be linear and there may be a plateau representing the optimal superpixel size at which point the best compromise of variability and size occurs. Figure 10 demonstrates the percentage of outliers at individual superpixels, as a proxy for variability, in the above study as a function of GCIPL thickness at superpixels.[22] The GCIPL's variability increased only when the thickness approached the measurement floor (Figure 11). Variability was slightly higher for GCC as compared to GCIPL in this study.

DISCUSSION OF OUR FINDINGS AND THEIR RELEVANCE AND IMPLICATIONS

Within-session vs. between-session variability—As mentioned above, we have demonstrated that within-session variability is very small when measured across 3°×3° macular superpixels and does not exceed 3 μm after exclusion of a small percentage of outliers.[22] However, variability of thickness measurements does vary among different patients and hence, estimating measurement variability in individual eyes is of potential clinical interest. We herein report that most of the total variability of macular thickness measurements observed on multiple imaging sessions over a period of 3 months or less could be explained by within-session variability. We chose an upper limit of 3 months for carrying out the 3 sessions of imaging as glaucoma would be expected to remain stable in treated patients during such as short period of time. The between-session variability component was highest for the FMT (36%) compared with other parameters and was lowest

for GCL (8%). It is not quite clear why FMT thickness measurements demonstrated a higher between-session component as full thickness measurements are expected to be less prone to segmentation errors. Presence of blood vessels could potentially increase variability, but blood vessels are included in both GCC and FMT measurements. After removal of the outer rim of superpixels that are known to be more variable, the magnitude of variability was uniform across the macula (Figure 10). From a clinical point of view, these findings suggest that repeat baseline macular SD-OCT images can be performed in a single session to gauge the magnitude of variability in individual eyes and there is no need to acquire repeat images on multiple sessions. As the measurement variability is uniform in the central region of the macula consisting of the central 36 superpixels, one can obtain pooled eye-specific variability estimates based on repeat macular images at baseline and use those for optimizing detection of progression in individual eyes. The sum of within-session and between-session variability also tended to correlate with the average superpixels thickness and was highest for GCC and lowest for GCL. Although the difference in variability between various thickness parameters was statistically significant due to the high number of superpixels involved, the absolute average difference was very small and given the resolution of current SD-OCT devices is of uncertain clinical significance.

The comparative utility of various macular measures for detection of progression especially in advanced glaucoma is yet to be fully established. With worsening glaucoma, inner retinal layers thin out, tissue density and density gradients diminish, and measurement accuracy decreases as segmentation algorithms are more likely to fail; hence, in more severe stages of glaucoma, FMT or GCC outcome measures may be more useful for detection of changes in thickness over time. Understandably, when the disease approaches the end stage, all structural data will lose their utility and detection of progression will have to rely only on functional approaches

Longitudinal structure-function relationships and their variability—Most previous studies pooled cross-sectional data from glaucoma (and normal) subjects to estimate the strength of SF relationships. As such, it is not clear how much of the total variability in this setting can be attributed to within-eye as opposed to between-individual components; a recent study found that variability was similar in glaucoma patients and normal subjects, suggesting that inter-individual variability constitutes a large fraction of total variability seen in cross-sectional SF studies.[77] Macular thickness measurements provide us with an opportunity to directly explore such SF relationships in individual eyes as the macular SD-OCT measurement cube and the central 10-degree VFs produce numerous measurements around the fovea or the fixation point; the SF relationships at equidistance regions of the macula and visual fields are expected to display similar patterns.

Studying SF relationships in *individual* glaucoma patients has been challenging due to the following reasons: a) the limited amount of data available from each eye cross-sectionally; b) the significant variability of neuroretinal rim and cpRNFL measurements in and around the optic nerve head reaching peaks and troughs that do not have corresponding variations in VF sensitivity measurements; and c) issues related to exact topographic matching of cpRNFL or neuroretinal rim measures and functional data in individual eyes.[78,79] Studying longitudinal SF relationships between macular thickness and central VF sensitivities

addresses most of these limitations: there are multiple SF measurements at comparable eccentricities in relation to the fovea; also, the relationship of macular superpixels and central VF threshold sensitivity measurements is for most part one to one after adjusting for the RGC displacement around the fovea, although such corrections are done for the average eye.[80]

We used multiple measurements taken over time in each individual eye to plot SF relationships as a function of distance from the fovea. We assumed that the 'true' relationship between macular GCIPL thickness derived from SD-OCT and corresponding VF sensitivities in individual eyes did not change over time regardless of disease stability or progression. We hypothesized that by combining multiple structural and functional measurements taken over time from the same eye, the 'true' relationship could be modeled more accurately given the larger number of data points available. As there were only 4 corresponding superpixel/TD values available at each exam at 3.4° eccentricity, we required at least 4 exams to be available in contrast to the 3 required exams for data at 5.6° and 6.8° eccentricities.

Our findings could be summarized as follows: 1) Within-eye variability in SF relationships is significantly less than between-patient variability regardless of distance from the fovea/fixation point; therefore, our approach should be able to more accurately estimate the SF parameters in individual eyes; 2) the broken-stick model could be fit for a majority of eyes at 5.6° and 6.8° eccentricities whereas it could be fit in less than half the superpixels/test locations at 3.4°; this is likely related to the small sample size per eye; 3) differences were found in structural measurement floor as a function of eccentricity and may exist in SF slopes; and 4) structure-function relationships seem to remain stable over time within individual eyes, i.e., no session-slope interaction was evident.

We used GCIPL thickness as the structural parameter of choice, since it is one of the best performing macular parameters for detection of early glaucoma and demonstrates the highest local correlation with VF TD values.[23] We used the logarithm of GCIPL as studying SF relationship on the same scale as VFs could result in stronger correlations than log-linear correlations.[44] As expected, the relationship between logGCIPL thickness and TD measurements was linear beyond the change point.

A question of interest is whether the SF relationships (including the slopes, intercepts and break points) follow a Gaussian distribution, i.e., whether there is evidence that the joint SF parameters in these eyes belong to a bigger family of normally-distributed parameters and variations seen in individual eyes merely represent measurement noise. We found that some of the aforementioned joint SF parameters at various eccentricities were not typically distributed in a Gaussian fashion (data not shown). Although our study was not powered nor tailored to address this question, the lack of a normal distribution for some parameters suggests the possibility that in contrast to what one would have expected, true differences in SF relationships may exist between individuals. This is a topic of significant interest and we plan to carry out future studies to better clarify this issue.

Both the neuroretinal rim and cpRNFL measurements reach their measurement floor in moderately advanced glaucoma and their clinical utility significant diminishes in the later stages of glaucoma.[63] On the other hand, macular structural measurements demonstrate residual thickness at later stages of the disease and therefore, are of potential interest for detection of progression in all stages of the disease including advanced glaucoma. Studying individual-eye macular SF relationships will facilitate better understanding and modeling of the inherent variability in these relationships across the spectrum of disease severity. We hypothesize that the longitudinal study of within-eye SF relationships can potentially be helpful for monitoring disease progression by combining, in a simple way, changes in the structural and functional data gleaned over time. Combining structure and function is a topic of significant interest in glaucoma.[81,82] While various approaches, such as Bayesian methods, have been explored, our proposed technique provides a simple method for simultaneous consideration of both structural and functional changes in a model that can be implemented in real time in the clinic and updated at each visit in an automated fashion. We hypothesize that downward and/or leftward movement of points along the modeled SF curve would represent disease deterioration, if confirmed over time and if consistent along both structural and functional axes. Figure 12 shows a scatter plot of superpixel thickness against VF TD values for a study eye at baseline and after 3 years of follow-up. A large number of data points moved down- and leftward after 3 years of follow-up; this highly suggests that this eye was deteriorating in both structural and functional domains during the follow-up period.

The results of the current study need to be interpreted in the light of the limitations. This approach requires a large number of corresponding structural and functional measurements for a given eye over time. A formal power calculation was elusive as there are differences in the magnitude of SF variability in individual eyes. The fact that we were able to fit the broken-stick model in less than half of eyes at 3.4° eccentricity probably reflects the lower sample size at this eccentricity as there were only 4 superpixels/test locations available per session. A broken-stick model can be fit only if SF measurements in an individual eye extend through most of the dynamic range of both structural and functional measurements. Only a median of 4 VF/OCT images per eye were available for this study. This may have limited the power of some of our analyses. We are planning a follow-up study that would address this topic after all study eyes have had 5 years of follow-up. From a diagnostic point of view, at some point during the course of the disease, all structural data will lose their utility and detection of progression will have to rely only on perimetric or other functional approaches.

CONCLUSION

The published literature provides strong evidence in favor of the utility of measuring central structure-function relationships in glaucoma. We demonstrate that acquiring repeat macular SD-OCT measurements within a single (baseline) session is adequate to estimate longitudinal variability in an individual eye over time. This finding has important implications with regard to designing algorithms to optimize macular OCT imaging for monitoring glaucoma.

Our study also demonstrates that longitudinal within-eye SF relationships have lower variability than those derived from pooled eyes and introduces the study of longitudinal within-eye SF relationships as a new concept for better understanding the relationship between macular RGC axonal complex and the corresponding functional measurements of the visual pathways. The proposed approach would potentially improve our understanding of the linking of structure-function in glaucoma and help refine progression algorithms based on macular and central VF measurements. More sensitive and reliable detection of glaucoma progression would allow for better monitoring of the effectiveness of treatment and guide clinicians as to when more aggressive treatment may be required.

Supplementary Material

Refer to Web version on PubMed Central for supplementary material.

ACKNOWLEDGMENT

A. *Funding/Support:* This study was supported by an unrestricted Departmental Grant from Research to Prevent Blindness and an unrestricted grant from Heidelberg Engineering and an NIH K23 grant (K23EY022659, KNM).

B. *Financial Disclosures:* Heidelberg Engineering (KNM, software and hardware support, unrestricted grant, honorarium)

C. *Contributions of Authors:*

- **a.** Kouros Nouri-Mahdavi, MD, MS: study design, data analyses, manuscript preparation
- **b.** Nima Fatehi, MD: data collection, analyses, manuscript review
- **c.** Joseph Caprioli, MD: review of results and manuscript

D. *Other Acknowledgments:* Jeff Gornbein DrPH, statistical consultant, SBCC Director, UCLA Department of Biomathematics, provided statistical expertise.

BIBLIOGRAPHY

1. Bourne RR, Taylor HR, Flaxman SR, et al. Number of people blind or visually impaired by glaucoma worldwide and in world regions 1990 – 2010: a meta-analysis. PLoS One. 2016;11(10):e0162229. [PubMed: 27764086]
2. Bogunović H, Kwon YH, Rashid A, et al. Relationships of retinal structure and humphrey 24–2 visual field thresholds in patients with glaucoma. Invest Ophthalmol Vis Sci. 1 2015;56(1):259–271.
3. Malik R, Swanson WH, Garway-Heath DF. ‘Structure-function relationship’ in glaucoma: past thinking and current concepts. Clin Exp Ophthalmol. May-Jun 2012;40(4):369–380. [PubMed: 22339936]
4. Quigley HA, Addicks EM, Green WR. Optic nerve damage in human glaucoma. III. Quantitative correlation of nerve fiber loss and visual field defect in glaucoma, ischemic neuropathy, papilledema, and toxic neuropathy. Arch Ophthalmol. 1 1982;100(1):135–146. [PubMed: 7055464]
5. Miglior S, Zeyen T, Pfeiffer N, et al. Results of the European Glaucoma Prevention Study. Ophthalmology. 3 2005;112(3):366–375. [PubMed: 15745761]
6. Stamper RL. The effect of glaucoma on central visual function. Trans Am Ophthalmol Soc. 1984;82:792–826. [PubMed: 6398938]
7. Zeimer R, Asrani S, Zou S, Quigley H, Jampel H. Quantitative detection of glaucomatous damage at the posterior pole by retinal thickness mapping. A pilot study. Ophthalmology 2 1998;105(2):224–231. [PubMed: 9479279]
8. CA C, KA A. Topography of ganglion cells in human retina. 1990.

9. Wassle H, Grunert U, Rohrenbeck J, Boycott BB. Cortical magnification factor and the ganglion cell density of the primate retina. Nature. 10 19 1989;341(6243):643–646. [PubMed: 2797190]
10. Hood DC, Raza AS, de Moraes CG, Johnson CA, Liebmann JM, Ritch R. The Nature of Macular Damage in Glaucoma as Revealed by Averaging Optical Coherence Tomography Data. Transl Vis Sci Technol. 5 2012;1(1):3.
11. Lisboa R, Leite MT, Zangwill LM, Tafreshi A, Weinreb RN, Medeiros FA. Diagnosing preperimetric glaucoma with spectral domain optical coherence tomography. Ophthalmology. 11 2012;119(11):2261–2269. [PubMed: 22883689]
12. Asrani S, Rosdahl JA, Allingham RR. Novel software strategy for glaucoma diagnosis: asymmetry analysis of retinal thickness. Arch Ophthalmol. 9 2011;129(9):1205–1211. [PubMed: 21911669]
13. Belghith A, Medeiros FA, Bowd C, et al. Structural Change Can Be Detected in Advanced-Glaucoma Eyes. Invest Ophthalmol Vis Sci. 7 01 2016;57(9):Oct511–518. [PubMed: 27454660]
14. Tan O, Chopra V, Lu AT, et al. Detection of macular ganglion cell loss in glaucoma by Fourier-domain optical coherence tomography. Ophthalmology. 12 2009;116(12):2305–2314 e2301–2302. [PubMed: 19744726]
15. Mwanza JC, Durbin MK, Budenz DL, et al. Glaucoma diagnostic accuracy of ganglion cell-inner plexiform layer thickness: comparison with nerve fiber layer and optic nerve head. Ophthalmology. 6 2012;119(6):1151–1158. [PubMed: 22365056]
16. Nouri-Mahdavi K, Nowroozizadeh S, Nassiri N, et al. Macular ganglion cell/inner plexiform layer measurements by spectral domain optical coherence tomography for detection of early glaucoma and comparison to retinal nerve fiber layer measurements. Am J Ophthalmol. 12 2013;156(6): 1297–1307.e1292. [PubMed: 24075422]
17. Shin HY, Park HY, Jung KI, Choi JA, Park CK. Glaucoma diagnostic ability of ganglion cell-inner plexiform layer thickness differs according to the location of visual field loss. Ophthalmology. 1 2014;121(1):93–99. [PubMed: 23962652]
18. Shin HY, Park HY, Jung KI, Park CK. Comparative study of macular ganglion cell-inner plexiform layer and peripapillary retinal nerve fiber layer measurement: structure-function analysis. Invest Ophthalmol Vis Sci. 11 08 2013;54(12):7344–7353. [PubMed: 24130187]
19. Zhang C, Tatham AJ, Weinreb RN, et al. Relationship between ganglion cell layer thickness and estimated retinal ganglion cell counts in the glaucomatous macula. Ophthalmology. 12 2014;121(12):2371–2379. [PubMed: 25148790]
20. Raza AS, Hood DC. Evaluation of the Structure-Function Relationship in Glaucoma Using a Novel Method for Estimating the Number of Retinal Ganglion Cells in the Human Retina. Invest Ophthalmol Vis Sci. 8 2015;56(9):5548–5556. [PubMed: 26305526]
21. Johnson CA, Sample PA, Cioffi GA, Liebmann JR, Weinreb RN. Structure and function evaluation (SAFE): I. criteria for glaucomatous visual field loss using standard automated perimetry (SAP) and short wavelength automated perimetry (SWAP). Am J Ophthalmol. 8 2002;134(2):177–185. [PubMed: 12140023]
22. Miraftabi A, Amini N, Gornbein J, et al. Local Variability of Macular Thickness Measurements With SD-OCT and Influencing Factors. Transl Vis Sci Technol. 7 2016;5(4):5.
23. Miraftabi A, Amini N, Morales E, et al. Macular SD-OCT Outcome Measures: Comparison of Local Structure-Function Relationships and Dynamic Range. Invest Ophthalmol Vis Sci. 9 01 2016;57(11):4815–4823. [PubMed: 27623336]
24. Drasdo N, Millican CL, Katholi CR, Curcio CA. The length of Henle fibers in the human retina and a model of ganglion receptive field density in the visual field. Vision Res. 10 2007;47(22): 2901–2911. [PubMed: 17320143]
25. Raza AS, Cho J, de Moraes CG, et al. Retinal ganglion cell layer thickness and local visual field sensitivity in glaucoma. Arch Ophthalmol. 12 2011;129(12):1529–1536. [PubMed: 22159673]
26. Hood DC, Kardon RH. A framework for comparing structural and functional measures of glaucomatous damage. Prog Retin Eye Res. 11 2007;26(6):688–710. [PubMed: 17889587]
27. Mwanza JC, Kim HY, Budenz DL, et al. Residual and dynamic range of retinal nerve fiber layer thickness in glaucoma: Comparison of three OCT platforms. Invest Ophthalmol Vis Sci. 10 2015;56(11):6344–6351. [PubMed: 26436887]

28. Amini N, Daneshvar R, Sharifipour F, et al. Structure-Function Relationships in Perimetric Glaucoma: Comparison of Minimum-Rim Width and Retinal Nerve Fiber Layer Parameters. Invest Ophthalmol Vis Sci. 9 1 2017;58(11):4623–4631. [PubMed: 28898356]
29. Miglior S, Riva I, Guareschi M, et al. Retinal sensitivity and retinal nerve fiber layer thickness measured by optical coherence tomography in glaucoma. Am J Ophthalmol. 11 2007;144(5):733–740. [PubMed: 17707327]
30. Racette L, Medeiros FA, Bowd C, Zangwill LM, Weinreb RN, Sample PA. The impact of the perimetric measurement scale, sample composition, and statistical method on the structure-function relationship in glaucoma. J Glaucoma. 12 2007;16(8):676–684. [PubMed: 18091454]
31. Gonzalez-Hernandez M, Pablo LE, Armas-Dominguez K, de la Vega RR, Ferreras A, de la Rosa MG. Structure-function relationship depends on glaucoma severity. Br J Ophthalmol. 9 2009;93(9):1195–1199. [PubMed: 19493858]
32. Lee JR, Jeoung JW, Choi J, Choi JY, Park KH, Kim YD. Structure-function relationships in normal and glaucomatous eyes determined by time- and spectral-domain optical coherence tomography. Invest Ophthalmol Vis Sci. 12 2010;51(12):6424–6430. [PubMed: 20592233]
33. Rao HL, Zangwill LM, Weinreb RN, Leite MT, Sample PA, Medeiros FA. Structure-function relationship in glaucoma using spectral-domain optical coherence tomography. Arch Ophthalmol. 7 2011;129(7):864–871. [PubMed: 21746976]
34. Nilforushan N, Nassiri N, Moghimi S, et al. Structure-Function Relationships between Spectral-Domain OCT and Standard Achromatic Perimetry. Investigative Ophthalmology & Visual Science. 5 2012 2012;53(6):2740–2748. [PubMed: 22447869]
35. Raza AS, Zhang X, De Moraes CG, et al. Improving glaucoma detection using spatially correspondent clusters of damage and by combining standard automated perimetry and optical coherence tomography. Invest Ophthalmol Vis Sci. 1 2014;55(1):612–624. [PubMed: 24408977]
36. Pollet-Villard F, Chiquet C, Romanet JP, Noel C, Aptel F. Structure-function relationships with spectral-domain optical coherence tomography retinal nerve fiber layer and optic nerve head measurements. Invest Ophthalmol Vis Sci. 5 02 2014;55(5):2953–2962. [PubMed: 24692125]
37. Ballae Ganeshrao S, Turpin A, Denniss J, McKendrick AM. Enhancing Structure-Function Correlations in Glaucoma with Customized Spatial Mapping. Ophthalmology. 8 2015;122(8):1695–1705. [PubMed: 26077579]
38. Danthurebandara VM, Sharpe GP, Hutchison DM, et al. Enhanced structure-function relationship in glaucoma with an anatomically and geometrically accurate neuroretinal rim measurement. Invest Ophthalmol Vis Sci. 1 2015;56(1):98–105.
39. Medeiros FA, Lisboa R, Weinreb RN, Girkin CA, Liebmann JM, Zangwill LM. A combined index of structure and function for staging glaucomatous damage. Arch Ophthalmol. 5 2012;130(5):E1–10. [PubMed: 22826832]
40. Medeiros FA, Zangwill LM, Anderson DR, et al. Estimating the rate of retinal ganglion cell loss in glaucoma. Am J Ophthalmol. 11 2012;154(5):814–824 e811. [PubMed: 22840484]
41. Meira-Freitas D, Lisboa R, Tatham A, et al. Predicting progression in glaucoma suspects with longitudinal estimates of retinal ganglion cell counts. Invest Ophthalmol Vis Sci. 6 19 2013;54(6):4174–4183. [PubMed: 23661375]
42. Tatham AJ, Weinreb RN, Medeiros FA. Strategies for improving early detection of glaucoma: the combined structure-function index. Clin Ophthalmol. 2014;8:611–621. [PubMed: 24707166]
43. Zhang C, Tatham AJ, Daga FB, Jammal AA, Medeiros FA. Event-based analysis of visual field change can miss fast glaucoma progression detected by a combined structure and function index. Graefes Arch Clin Exp Ophthalmol. 7 2018;256(7):1227–1234. [PubMed: 29623461]
44. Garway-Heath DF, Caprioli J, Fitzke FW, Hitchings RA. Scaling the hill of vision: the physiological relationship between light sensitivity and ganglion cell numbers. Invest Ophthalmol Vis Sci. 6 2000;41(7):1774–1782. [PubMed: 10845598]
45. Garway-Heath DF, Holder GE, Fitzke FW, Hitchings RA. Relationship between electrophysiological, psychophysical, and anatomical measurements in glaucoma. Invest Ophthalmol Vis Sci. 7 2002;43(7):2213–2220. [PubMed: 12091419]

46. Swanson WH, Felius J, Pan F. Perimetric defects and ganglion cell damage: interpreting linear relations using a two-stage neural model. Invest Ophthalmol Vis Sci. 2 2004;45(2):466–472. [PubMed: 14744886]
47. Pan F, Swanson WH. A cortical pooling model of spatial summation for perimetric stimuli. J Vis. 2006;6(11):1159–1171. [PubMed: 17209726]
48. Drasdo N, Mortlock KE, North RV. Ganglion cell loss and dysfunction: relationship to perimetric sensitivity. Optom Vis Sci. 11 2008;85(11):1036–1042. [PubMed: 18981918]
49. Harwerth RS, Wheat JL, Fredette MJ, Anderson DR. Linking structure and function in glaucoma. Prog Retin Eye Res. 7 2010;29(4):249–271. [PubMed: 20226873]
50. Harwerth RS, Carter-Dawson L, Shen F, Smith EL, 3rd, Crawford ML. Ganglion cell losses underlying visual field defects from experimental glaucoma. Invest Ophthalmol Vis Sci. 9 1999;40(10):2242–2250. [PubMed: 10476789]
51. Ohkubo S, Higashide T, Udagawa S, et al. Focal relationship between structure and function within the central 10 degrees in glaucoma. Invest Ophthalmol Vis Sci. 8 2014;55(8):5269–5277. [PubMed: 25082882]
52. Rao HL, Januwada M, Hussain RS, et al. Comparing the Structure-Function Relationship at the Macula With Standard Automated Perimetry and Microperimetry. Invest Ophthalmol Vis Sci. 12 2015;56(13):8063–8068. [PubMed: 26720457]
53. Sato S, Hirooka K, Baba T, Tenkumo K, Nitta E, Shiraga F. Correlation between the ganglion cell-inner plexiform layer thickness measured with cirrus HD-OCT and macular visual field sensitivity measured with microperimetry. Invest Ophthalmol Vis Sci. 4 30 2013;54(4):3046–3051. [PubMed: 23580483]
54. Le PV, Tan O, Chopra V, et al. Regional correlation among ganglion cell complex, nerve fiber layer, and visual field loss in glaucoma. Invest Ophthalmol Vis Sci. 6 21 2013;54(6):4287–4295. [PubMed: 23716631]
55. Kim S, Lee JY, Kim SO, Kook MS. Macular structure-function relationship at various spatial locations in glaucoma. Br J Ophthalmol. 10 2015;99(10):1412–1418. [PubMed: 25829487]
56. Lee JW, Morales E, Sharifipour F, et al. The relationship between central visual field sensitivity and macular ganglion cell/inner plexiform layer thickness in glaucoma. Br J Ophthalmol. 8 2017;101(8):1052–1058. [PubMed: 28077369]
57. Araie M, Saito H, Tomidokoro A, Murata H, Iwase A. Relationship between macular inner retinal layer thickness and corresponding retinal sensitivity in normal eyes. Invest Ophthalmol Vis Sci. 11 2014;55(11):7199–7205. [PubMed: 25301876]
58. Takagi ST, Kita Y, Yagi F, Tomita G. Macular retinal ganglion cell complex damage in the apparently normal visual field of glaucomatous eyes with hemifield defects. J Glaucoma. Jun-Jul 2012;21(5):318–325. [PubMed: 21423034]
59. Inuzuka H, Kawase K, Sawada A, Aoyama Y, Yamamoto T. Macular retinal thickness in glaucoma with superior or inferior visual hemifield defects. J Glaucoma. 1 2013;22(1):60–64. [PubMed: 21878820]
60. Curcio CA, Messinger JD, Sloan KR, Mitra A, McGwin G, Spaide RF. Human chorioretinal layer thicknesses measured in macula-wide, high-resolution histologic sections. Invest Ophthalmol Vis Sci. 6 06 2011;52(7):3943–3954. [PubMed: 21421869]
61. Hood DC, Anderson SC, Wall M, Kardon RH. Structure versus function in glaucoma: an application of a linear model. Invest Ophthalmol Vis Sci. 8 2007;48(8):3662–3668. [PubMed: 17652736]
62. Bowd C, Zangwill LM, Weinreb RN, Medeiros FA, Belghith A. Estimating Optical Coherence Tomography Structural Measurement Floors to Improve Detection of Progression in Advanced Glaucoma. Am J Ophthalmol. 3 2017;175:37–44. [PubMed: 27914978]
63. Sung KR, Sun JH, Na JH, Lee JY, Lee Y. Progression detection capability of macular thickness in advanced glaucomatous eyes. Ophthalmology. 2 2012;119(2):308–313. [PubMed: 22182800]
64. Na JH, Sung KR, Baek S, et al. Detection of glaucoma progression by assessment of segmented macular thickness data obtained using spectral domain optical coherence tomography. Invest Ophthalmol Vis Sci. 6 20 2012;53(7):3817–3826. [PubMed: 22562510]

65. Lee KS, Lee JR, Na JH, Kook MS. Usefulness of macular thickness derived from spectral-domain optical coherence tomography in the detection of glaucoma progression. Invest Ophthalmol Vis Sci. 3 2013;54(3):1941–1949. [PubMed: 23422822]

66. Suda K, Hangai M, Akagi T, et al. Comparison of Longitudinal Changes in Functional and Structural Measures for Evaluating Progression of Glaucomatous Optic Neuropathy. Invest Ophthalmol Vis Sci. 8 2015;56(9):5477–5484. [PubMed: 26284553]

67. Hammel N, Belghith A, Weinreb RN, Medeiros FA, Mendoza N, Zangwill LM. Comparing the Rates of Retinal Nerve Fiber Layer and Ganglion Cell-Inner Plexiform Layer Loss in Healthy Eyes and in Glaucoma Eyes. Am J Ophthalmol. 6 2017;178:38–50. [PubMed: 28315655]

68. Lee WJ, Kim YK, Park KH, Jeoung JW. Trend-based Analysis of Ganglion Cell-Inner Plexiform Layer Thickness Changes on Optical Coherence Tomography in Glaucoma Progression. Ophthalmology. 9 2017;124(9):1383–1391. [PubMed: 28412067]

69. Mwanza JC, Oakley JD, Budenz DL, Chang RT, Knight OJ, Feuer WJ. Macular ganglion cell-inner plexiform layer: automated detection and thickness reproducibility with spectral domain-optical coherence tomography in glaucoma. Invest Ophthalmol Vis Sci. 10 21 2011;52(11):8323–8329. [PubMed: 21917932]

70. Hirasawa H, Araie M, Tomidokoro A, et al. Reproducibility of thickness measurements of macular inner retinal layers using SD-OCT with or without correction of ocular rotation. Invest Ophthalmol Vis Sci. 4 05 2013;54(4):2562–2570. [PubMed: 23493298]

71. Tan O, Li G, Lu AT, Varma R, Huang D. Mapping of macular substructures with optical coherence tomography for glaucoma diagnosis. Ophthalmology. 6 2008;115(6):949–956. [PubMed: 17981334]

72. Kim NR, Kim JH, Lee J, Lee ES, Seong GJ, Kim CY. Determinants of perimacular inner retinal layer thickness in normal eyes measured by Fourier-domain optical coherence tomography. Invest Ophthalmol Vis Sci. 5 2011;52(6):3413–3418. [PubMed: 21357406]

73. Kim KE, Yoo BW, Jeoung JW, Park KH. Long-Term Reproducibility of Macular Ganglion Cell Analysis in Clinically Stable Glaucoma Patients. Invest Ophthalmol Vis Sci. 7 2015;56(8):4857–4864. [PubMed: 25829417]

74. Sohn EH, Chen JJ, Lee K, Niemeijer M, Sonka M, Abràmoff MD. Reproducibility of diabetic macular edema estimates from SD-OCT is affected by the choice of image analysis algorithm. Invest Ophthalmol Vis Sci. 6 2013;54(6):4184–4188. [PubMed: 23696607]

75. Liu X, Shen M, Huang S, Leng L, Zhu D, Lu F. Repeatability and reproducibility of eight macular intraretinal layer thicknesses determined by an automated segmentation algorithm using two SD-OCT instruments. PLoS One. 2014;9(2):e87996. [PubMed: 24505345]

76. Francoz M, Fenolland JR, Giraud JM, et al. Reproducibility of macular ganglion cell-inner plexiform layer thickness measurement with cirrus HD-OCT in normal, hypertensive and glaucomatous eyes. Br J Ophthalmol. 3 2014;98(3):322–328. [PubMed: 24307717]

77. Ashimatey BS, Swanson WH. Between-Subject Variability in Healthy Eyes as a Primary Source of Structural-Functional Discordance in Patients With Glaucoma. Invest Ophthalmol Vis Sci. 2 2016;57(2):502–507. [PubMed: 26873511]

78. Lamparter J, Russell RA, Zhu H, et al. The influence of intersubject variability in ocular anatomical variables on the mapping of retinal locations to the retinal nerve fiber layer and optic nerve head. Invest Ophthalmol Vis Sci. 9 2013;54(9):6074–6082. [PubMed: 23882689]

79. Garway-Heath DF, Poinoosawmy D, Fitzke FW, Hitchings RA. Mapping the visual field to the optic disc in normal tension glaucoma eyes. Ophthalmology. 10 2000;107(10):1809–1815. [PubMed: 11013178]

80. Turpin A, Chen S, Sepulveda JA, McKendrick AM. Customizing Structure-Function Displacements in the Macula for Individual Differences. Invest Ophthalmol Vis Sci. 9 2015;56(10):5984–5989. [PubMed: 26393464]

81. Medeiros FA, Leite MT, Zangwill LM, Weinreb RN. Combining structural and functional measurements to improve detection of glaucoma progression using Bayesian hierarchical models. Invest Ophthalmol Vis Sci. 7 2011;52(8):5794–5803. [PubMed: 21693614]

82. Russell RA, Malik R, Chauhan BC, Crabb DP, Garway-Heath DF. Improved estimates of visual field progression using bayesian linear regression to integrate structural information in patients

with ocular hypertension. Invest Ophthalmol Vis Sci. 5 2012;53(6):2760–2769. [PubMed: 22467579]

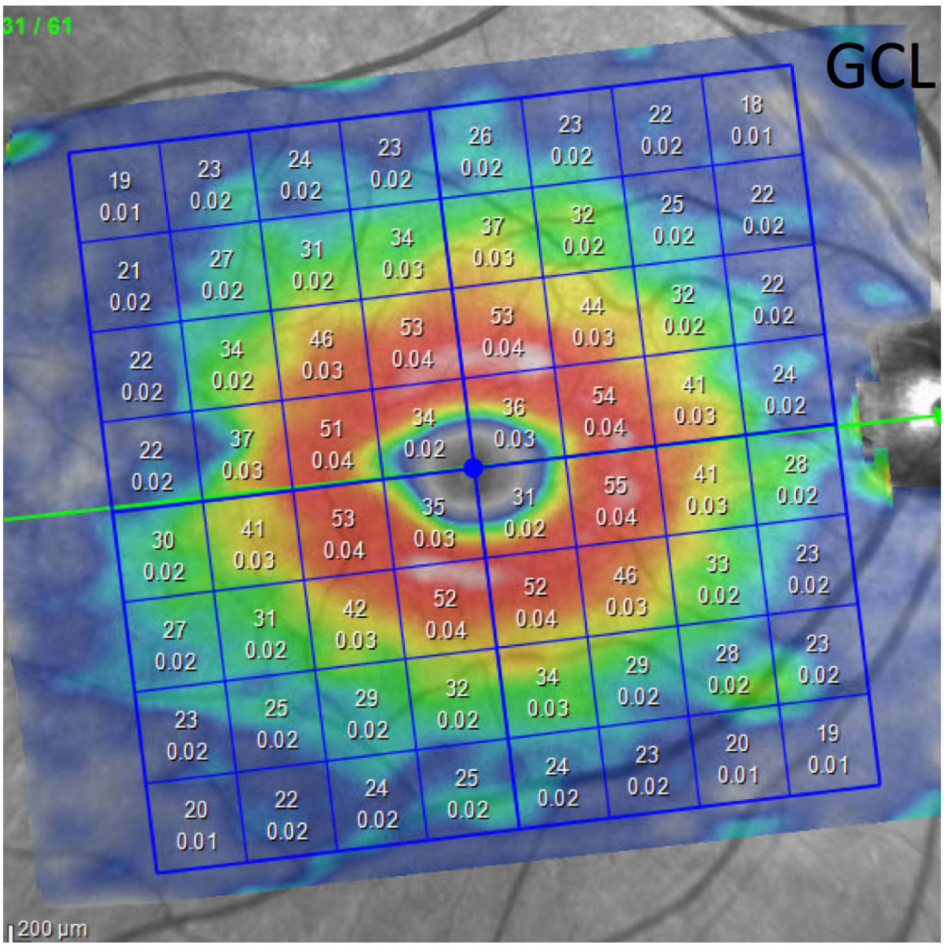

Figure 1.

An example of a macular image generated by the Spectralis spectral domain optical coherence tomography. The central 24° of the macular image is segmented, thickness measurements are calculated for individual retinal layers and data are presented as an 8×8 grid of superpixels 3°×3° in size. In this image, the top numbers in each superpixel represent ganglion cell layer thickness.

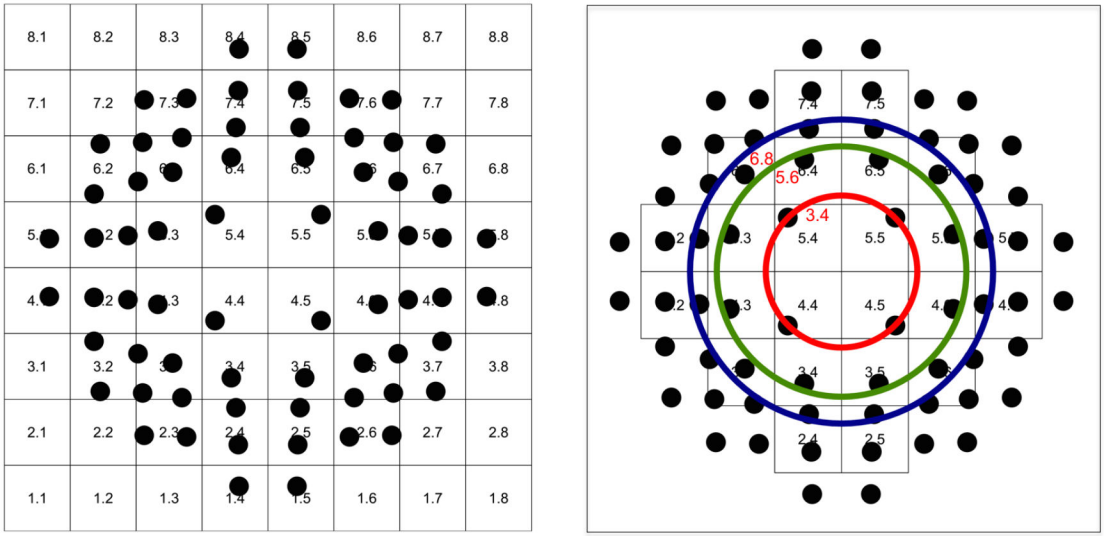

Figure 2.

Left, an anatomically accurate overlay of the test locations from the central 10° visual field (10–2 strategy) onto the macular 8×8 grid after adjusting for retinal ganglion cell displacement.[25] Right, circles demonstrate superpixels and visual field test locations at 3.4°, 5.6° and 6.8° eccentricities where the macular inner layer thickness is adequate so that accurate measurements can be carried out and structure-function relationships may be explored. The central 36 superpixels were included for the cross-sectional study, whereas only the central 24 superpixels were included for the longitudinal study.

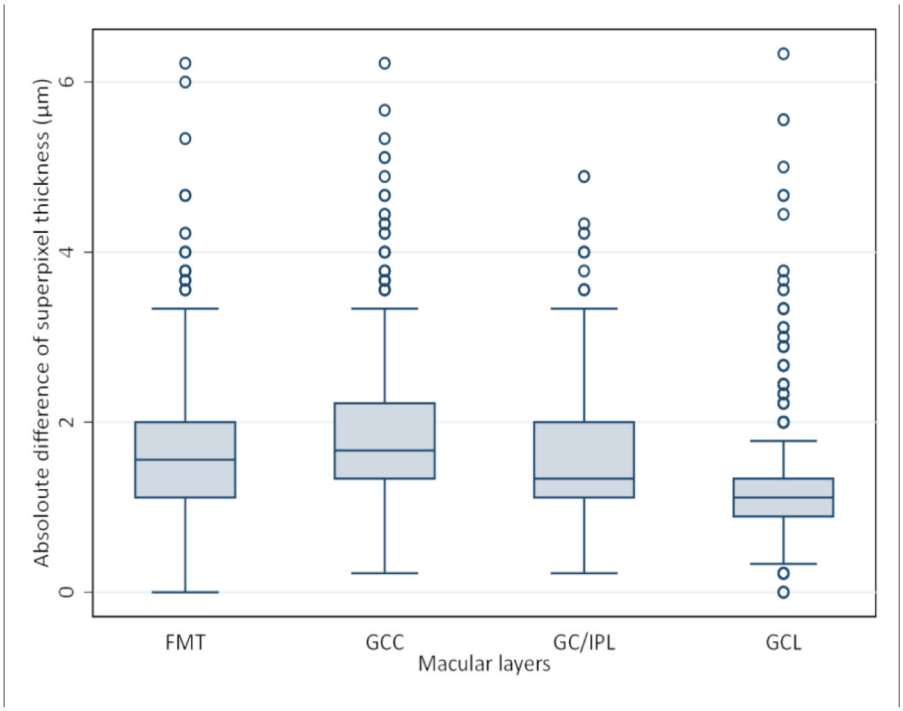

Figure 3.

Box plot shows the mean absolute difference of 9 repeat optical coherence tomography images (3 images per session and 3 sessions) at each superpixel for the macular outcomes of interest. The pairwise mean differences were statistically different among all four parameters (P <0.001, Kruskal-Wallis test). GCL, ganglion cell layer; GC/IPL, ganglion cell and inner plexiform layer; GCC, ganglion cell complex; FMT, full macular thickness.

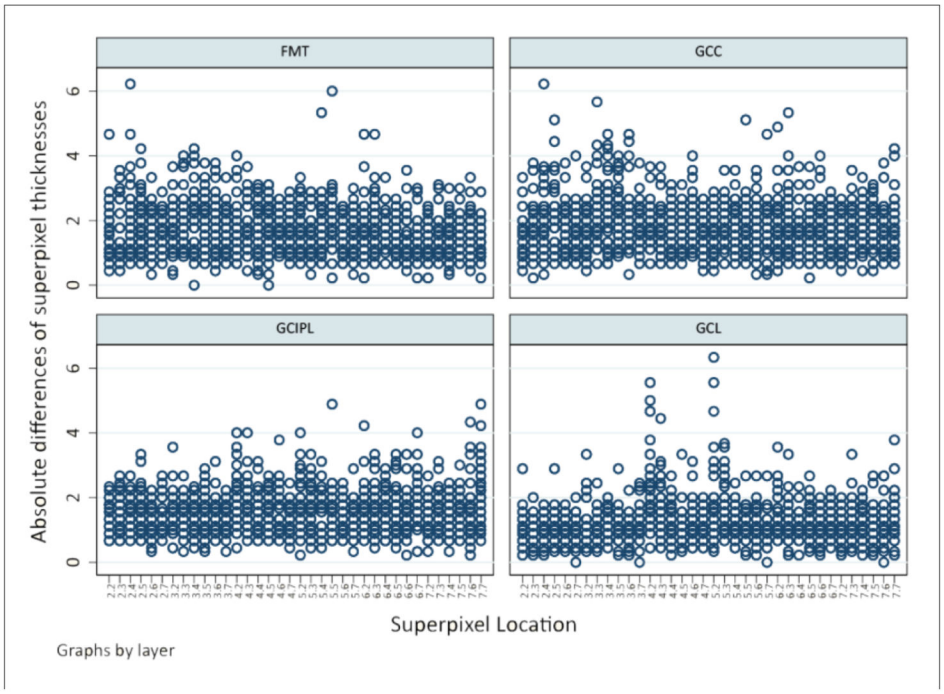

Figure 4.

Scatter plots demonstrating the variability of macular thickness measurements, expressed as the absolute differences in thickness among the 9 optical coherence tomography images (3 images per session over 3 sessions) as a function of superpixel location (on the X axis).

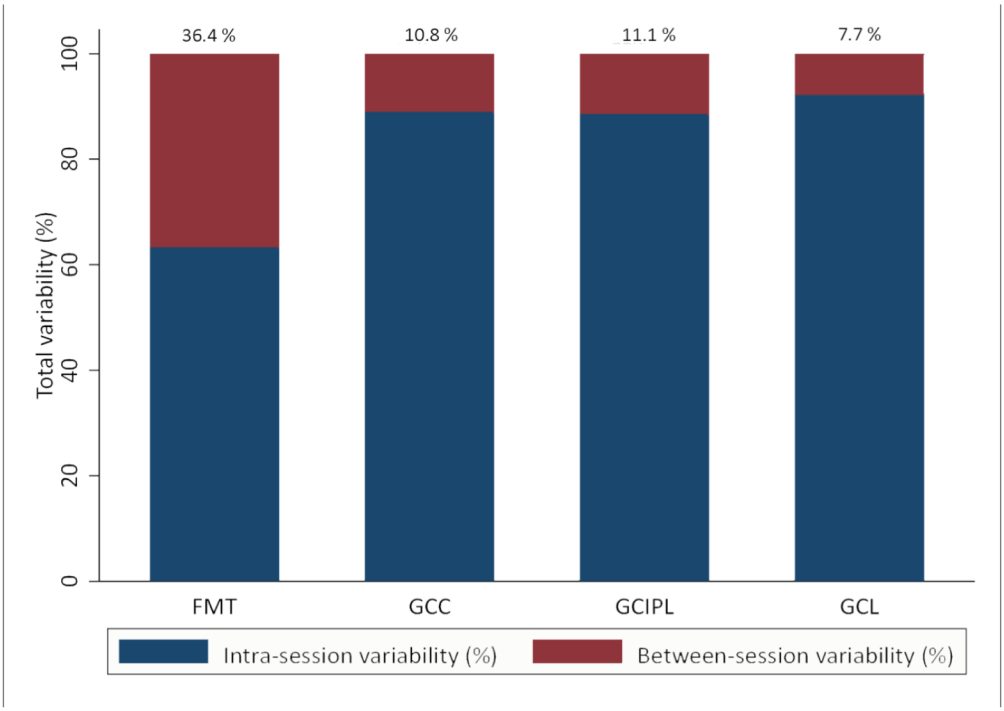

Figure 5.
Bar graph shows the contribution of the between-session and within-session variability to total variability of macular superpixel thickness measurements on 9 different imaging sessions.

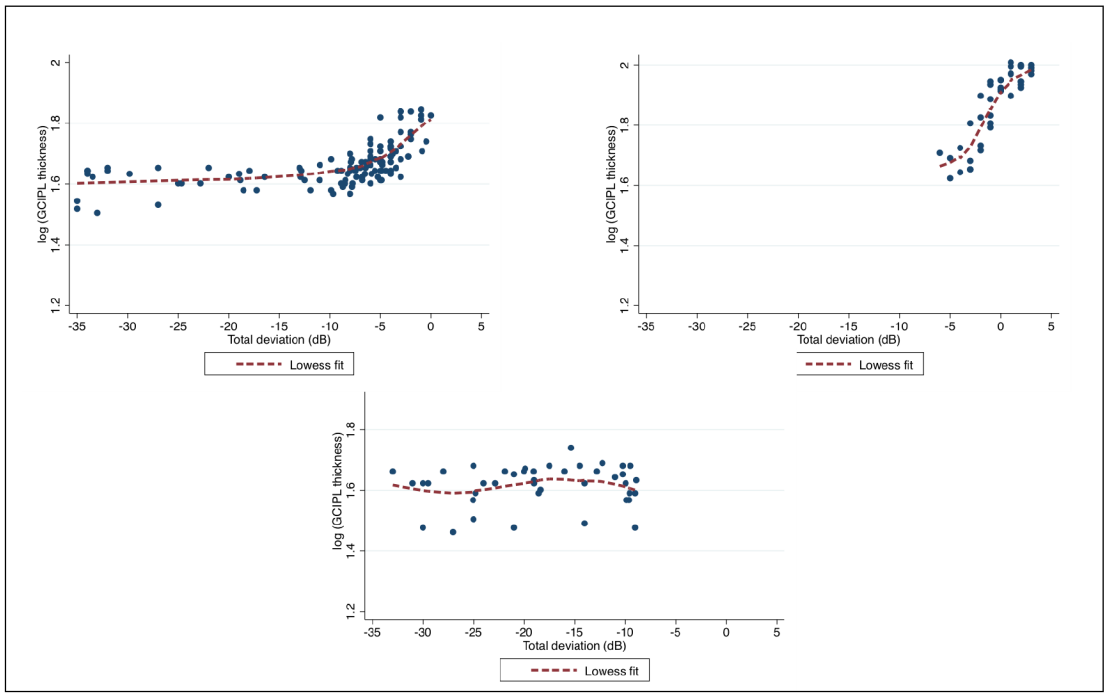

Figure 6.

Three patterns were observed after drawing bivariate plots of cross-sectional GCIPL and visual field (VF) total deviation measurements in individual eyes in the longitudinal study. Top left, a typical broken stick pattern is observed since both GCIPL thickness and VF sensitivity values vary through most or all of their entire range of measurements; top right, the GCIPL thickness measurements vary through most of their dynamic range, whereas there is limited variability in VF measurements, indicating only mild corresponding VF damage; bottom, the VF threshold values demonstrate a much wider range of variation in contrast to the GCIPL thickness measurements as the latter have reached their measurement floor.

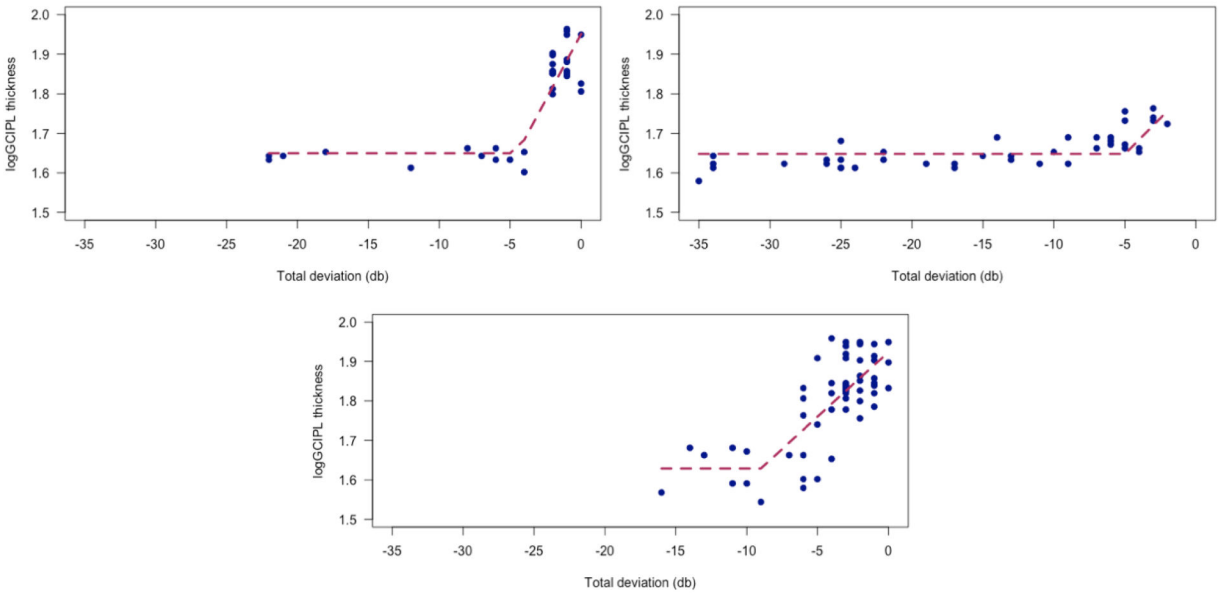

Figure 7.

Examples of longitudinal structure-function relationships in individual eyes. Top left, an eye with small variability in both macular thickness and 10–2 total deviation measurements over time. The change point was around −5 dB. Top right, fairly consistent SF relationships over multiple sessions with moderate variability. The change point is around −10 dB. Bottom, longitudinal SF plot for an eye, in which the TD values do not fall below −15 dB. The change point was estimated around −9 dB in this eye.

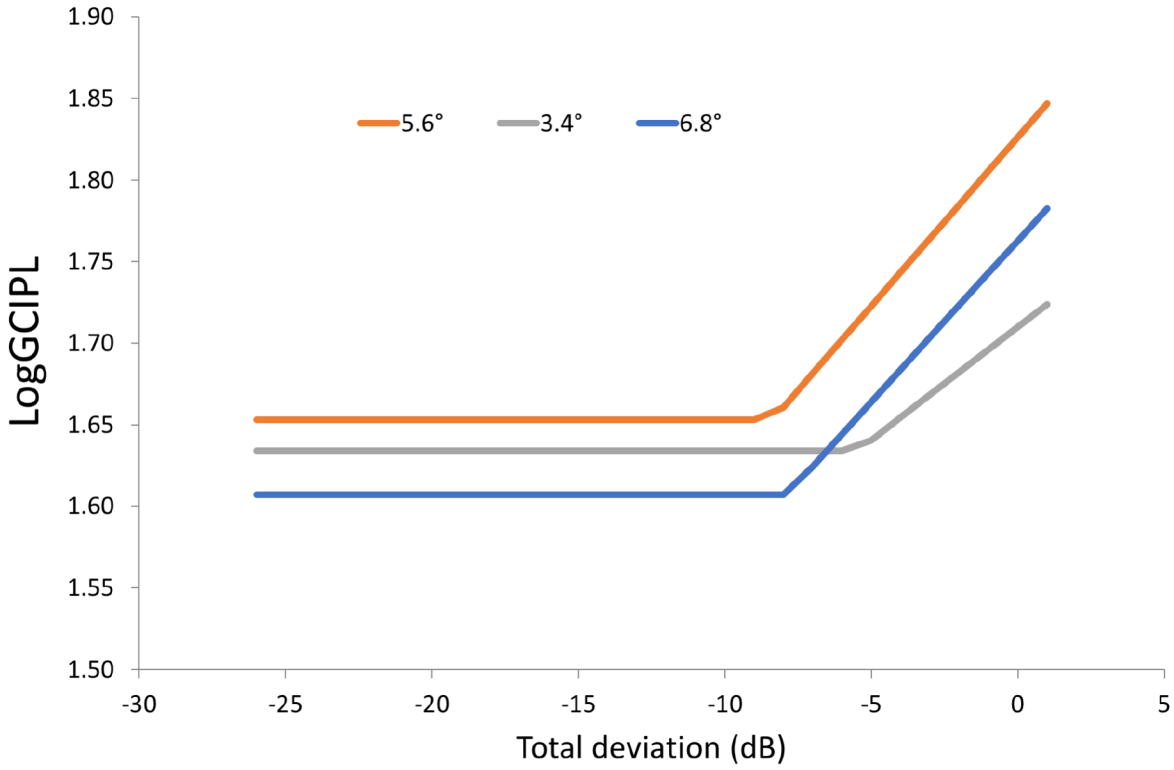

Figure 8.
Modeled relationship of the logGCIPL vs. total deviation values at corresponding 10–2 visual field locations as a function of eccentricity.

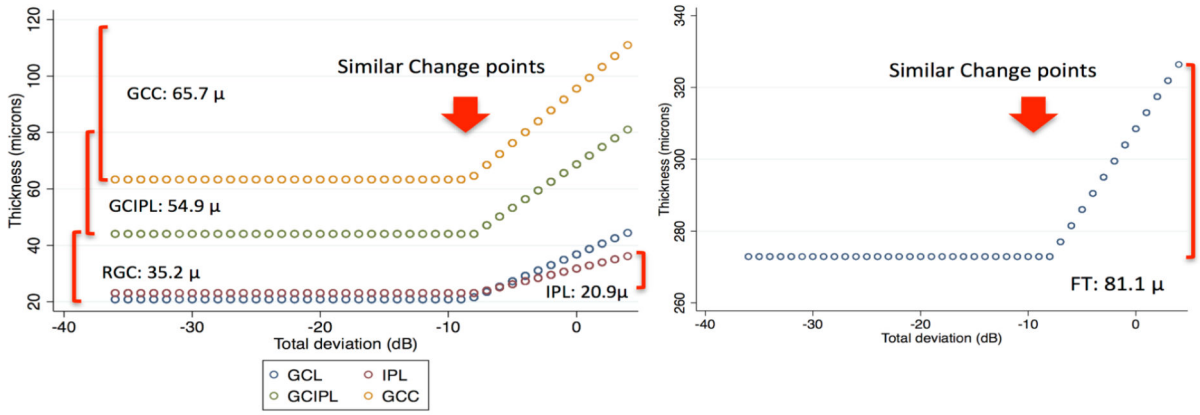

Figure 9.

The plots demonstrate the modeled relationship between macular thickness at 3°×3° superpixels and visual field total deviation based on a broken stick model. The thickness of the ganglion cell layer, ganglion cell/inner plexiform layers, ganglion cell complex, or full macular thickness within central 24 superpixels is represented on the Y axis; the total deviation at individual test locations of the 10–2 visual field is displayed on the X axis. The red arrows point to the change point for various macular outcome measures based on the broken stick model. The numbers represent the absolute dynamic range at 5.6° eccentricity. Please note that the absolute range increases as a function of the average thickness of the layers of interest in normal subjects. IPL, inner plexiform layer; GCL, ganglion cell layer; GCIPL, ganglion cell and inner plexiform layers; GCC, ganglion cell complex; FT, full macular thickness. (from Miraftabi A et al. Macular SD-OCT outcome measures: comparison of local structure-function relationships and dynamic range. *Invest Ophthalmol Vis Sci*. 2016 Sep 1;57(11):4815–23.)

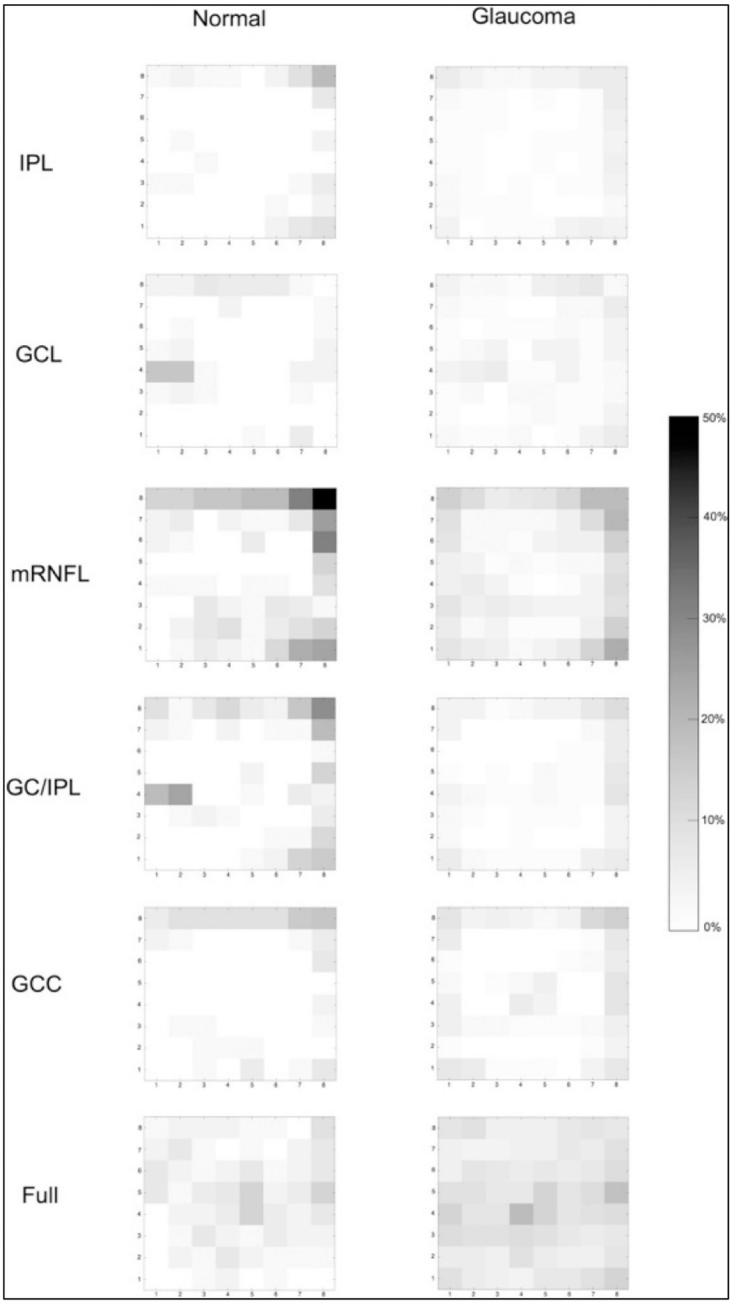

Figure 10.

The percentage of outliers at individual superpixels in a group of glaucoma and normal eyes, which had ×3 macular measurements within the same session, as a proxy for variability, for various macular outcome measures. Darker shades represent higher proportion of outliers. IPL, inner plexiform layer; GCL, ganglion cell layer; mRNFL, macular retinal nerve fiber layer; GC/IPL, ganglion cell and inner plexiform layer; GCC, ganglion cell complex; Full, full macular thickness. (from Miraftabi A et al. Local variability of macular thickness measurements with SD-OCT and influencing factors. *Transl Vis Sci Technol*. 2016 Jul 19;5(4):5.)

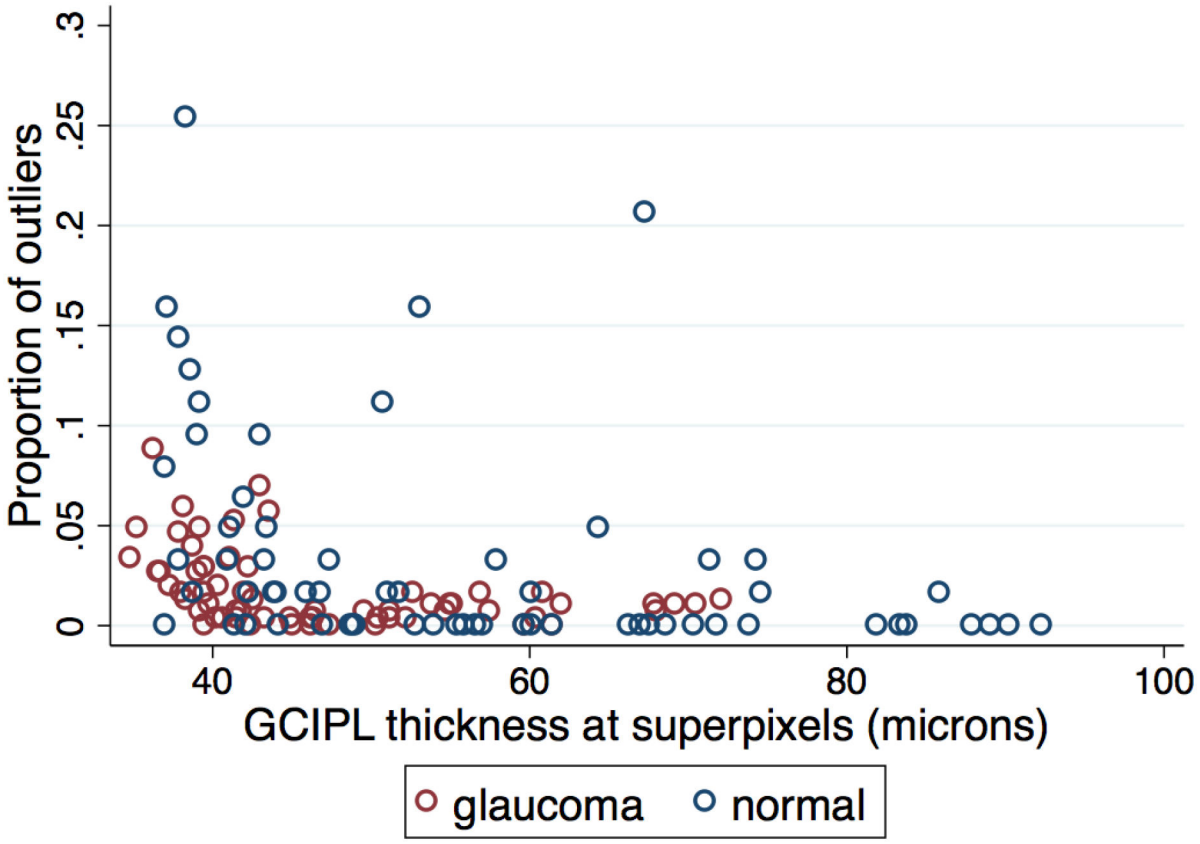

Figure 11.

Scatter plot displays the proportion of outliers (a proxy for within-session variability) for ganglion cell/inner plexiform layer (GCIPL) thickness at 3°×3° superpixels as a function of GCIPL thickness. GCIPL variability increased only when the thickness approached the measurement floor. (from Miraftabi A et al. Local variability of macular thickness measurements with SD-OCT and influencing factors. *Transl Vis Sci Technol*. 2016 Jul 19;5(4):5.)

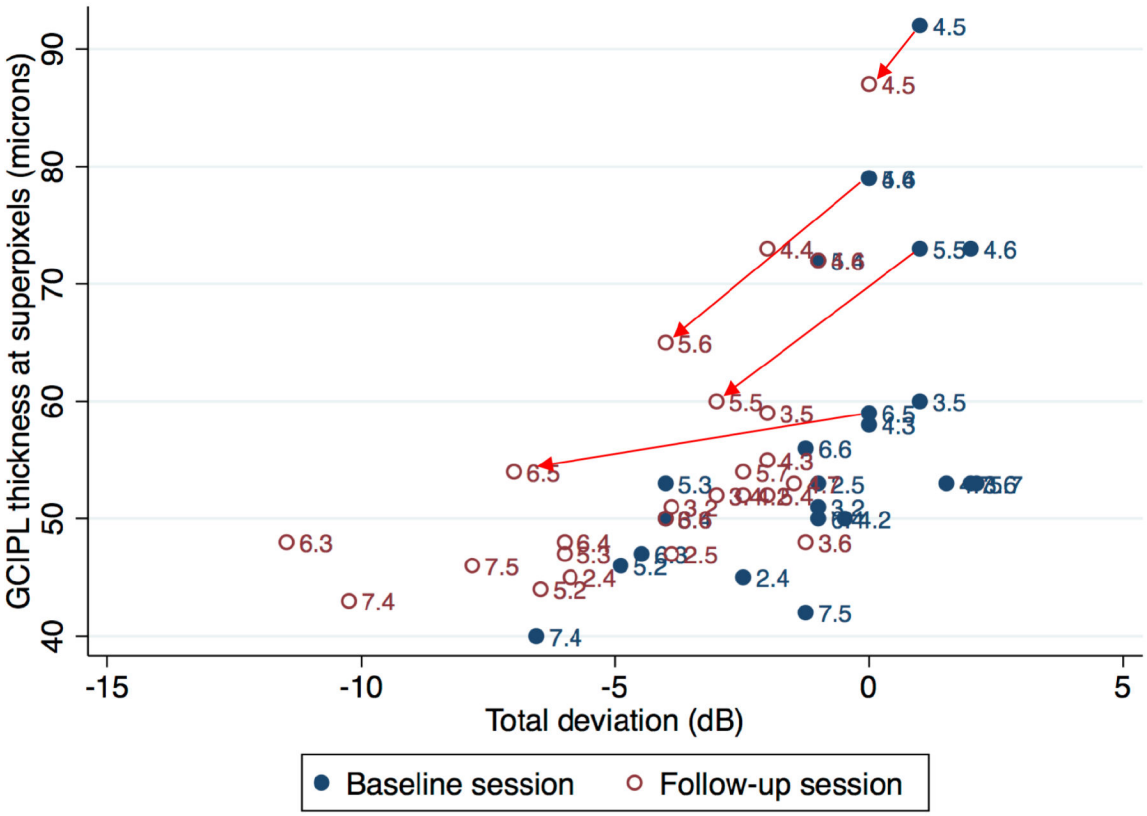

Figure 12.

Scatter plot of ganglion cell/inner plexiform layer (GCIPL) thickness (in microns) at macular 3°×3° superpixels vs. visual field total deviation values at corresponding test locations at baseline (blue full circles) and after 36 months of follow-up (maroon hollow circles) in an individual eye. A large number of points have moved left and down, an indication of worsening in both structural and functional domains. Arrows showcase a few examples of worsening macular superpixels and corresponding visual field test locations.

Table 1.

Demographic and clinical characteristics of the cross-sectional study sample.

	Glaucoma (26 eyes of 14 patients)	**Normal (12 eyes of 6 subjects)**
Age (median/interquartile range, years)	65.0 (56.2–72.3)	49.2 (40.4–49.2)
Gender (Female/Male)	7/7	4/2
Mean deviation (median/ interquartile range, dB)	−3.1 (−4.6 to-0.9)	0.5 (−1.4 to 1.1)
Visual acuity (median/ interquartile range, logMAR)	0.00 (−0.10 to 0.00)	0.00 (0.00 to 0.00)
Ethnicity		
White	6	3
Hispanic	2	3
Asian	4	0
African American	2	0

Table 2.

Demographic and clinical characteristics of the longitudinal study cohort.

Variables	
Age (median/ interquartile range, years)	56.6 (50.7–62.5)
Gender (Female/Male)	32/21
Ethnicity	
White	30
Asian	9
African-American	9
Hispanic	5
24–2 visual field mean deviation (median/ interquartile range, dB)	−8.3 (±5.0)
10–2 visual field mean deviation, average (±SD)(dB)	−9.7 (±4.9)
No. of imaging/visual field sessions per eye, median (interquartile range)	4 (4–6)
Follow-up time (median/interquartile range, years)	2.4 (2.2–2.9)

Table 3.

Results of segmented regression analyses in 53 eyes of patients who had macular imaging (with measurement of the ganglion cell/inner plexiform layer thickness) and central 10–2 visual field exams at 3 or more sessions during follow-up. The column 'Number of eyes' represents the number of eyes where the model could be fit.

	3.4° eccentricity (44 eyes)			
	Number of eyes	***Q1***	***Median***	***Q3***
Intercept	20	1.526	1.558	1.612
Slope	20	0.006	0.017	0.029
Break point	20	−21.22	−9.72	−6.22
	5.6° eccentricity (53 eyes)			
	Number of eyes	***Q1***	***Median***	***Q3***
Intercept	43	1.627	1.647	1.680
Slope	43	0.015	0.020	0.034
Break point	43	−13.93	−8.93	−6.68
	6.8° eccentricity (53 eyes)			
	Number of eyes	***Q1***	***Median***	***Q3***
Intercept	38	1.588	1.607	1.630
Slope	38	0.010	0.016	0.027
Break point	38	−12.98	−8.77	−7.25

P value <0.001 for all for comparison to zero; intercept = $a+b_0$, slope=b

Table 4.

The absolute and relative dynamic range (DR) for various macular outcomes of interest at 5.6° eccentricity. The ganglion cell layer demonstrated the largest relative dynamic range.

Parameter	Absolute DR (μm)	Average Thickness (jxm)	Relative DR
Ganglion cell layer	35.2	43.4	81%
Ganglion cell and inner plexiform layers	54.9	80.4	68%
Ganglion cell complex	65.7	105.5	62%
Full macular thickness	81.1	321.3	25%